Max-Planck-Institut
für Meteorologie

REPORT No. 45

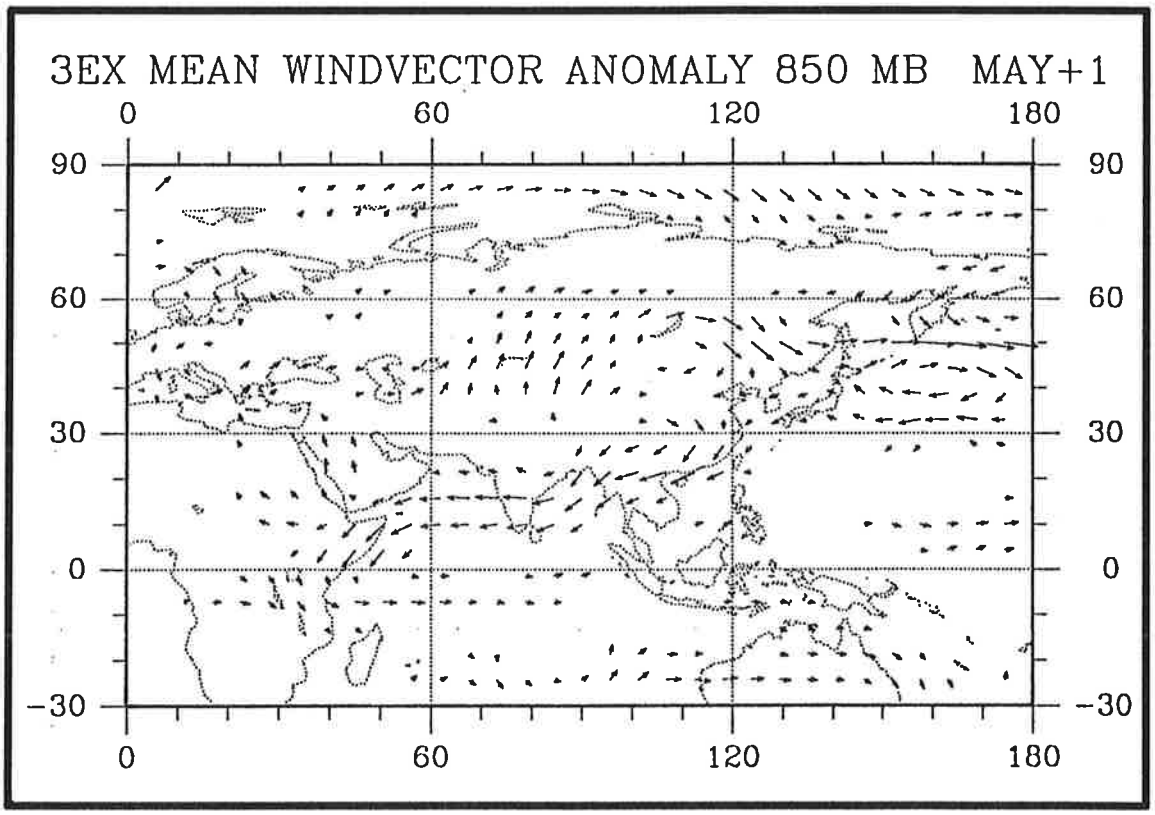

FORCED COOLING OF THE POLAR T21 ATMOSPHERE AND TROPICAL CLIMATE VARIABILITY

by

HANS-FRIEDRICH GRAF

HAMBURG, DECEMBER 1989

AUTHOR:

HANS-FRIEDRICH GRAF

HUMBOLDT UNIVERSITÄT ZU BERLIN
SEKTION PHYSIK
MÜGGELSEEDAMM 256
BERLIN 1162
GDR

MAX-PLANCK-INSTITUT
FUER METEOROLOGIE
BUNDESSTRASSE 55
D-2000 HAMBURG 13
F.R. GERMANY

Tel.: (040) 4 11 73-0
Telex: 211092
Telemail: MPI.Meteorology
Telefax: (040) 4 11 73-298

REPb45

Forced Cooling of the Polar T21 Atmosphere and Tropical Climate Variability

Hans-F. Graf

Humboldt Universität zu Berlin *
Sektion Physik

Müggelseedamm 256, Berlin 1162, GDR

*This paper was entirely completed during visits at the Max-Planck-Institut for Meteorology Hamburg, FRG

ISSN 0937-1060

Abstract:

One of the generally accepted climatic effects of stratospheric aerosol injection is the reduction of the global radiation in high latitudes by an order of 5% at El Chichon type eruptions . It is suggested that this radiation deficit is possible external forcing factor for the above-mentioned climatic anomalies associated with ENSO events. To test this hypothesis, the effect of high-latitude radiational forcing was examined in a GCM experiment. The results provide physically-consistent evidence in support of the basic hypothesis. The main supporting factor is the creation of enhanced snow cover in regions of Asia which are removed from the location of the introduced radiation anomaly. The simulated results show certain features, which are well known from observations in weak monsoon years, i.e. the weakened easterly jet in the upper troposphere over northern India, prolonged winter monsoon conditions and prevailing anticyclonal vorticity anomalies over the entire Indian summer monsoon region. Over the western Pacific at the end of boreal winter (May), increased convective activity leads to a negative Walker Circulation anomaly with westerly wind anomalies near the surface and easterly anomalies in the upper troposphere. This is known as one of the most important anomalies at the beginning of an ENSO event.

1. Introduction

Most of the variability of tropical climate is connected with variations of the Indian monsoon and of El Niño/Southern Oscillation. The basic process of the development of ENSO episodes involves quasi-periodic oscillations of the air pressure patterns over the southern Pacific and Indian Oceans (van Loon, 1984; van Loon and Shea, 1985, 1987; von Storch et al., 1987). These oscillations result in changes of the strength of the zonal Walker Circulation. A strong Walker Circulation (which normally is coupled with a strong Tahiti High and South-East Trades) leads to a positive sea-level anomaly in the western Pacific due to advected warm water at the surface. A decreasing easterly wind anomaly then triggers the relaxation of the sea-level anomaly by the redistribution of surplus water via the west-east directed equatorial currents and a Kelvin wave which crosses the Pacific basin taking several months to do so. These processes result in positive sea surface temperature anomalies, primarily off the South American Pacific Coast ("coastal" El Niños, Graf, 1986).

There may also be non-local processes that influence the Pacific Walker Circulation and thus may act as external (with respect to the coupled system *tropical ocean and atmosphere*) forcing factors for the auto-oscillation. They may hinder or promote the development of the auto-oscillation, depending on the phase relationships. These external forcing factors include cool episodes in higher latitudes of the northern hemisphere, which can influence the winds over the western equatorial Pacific ocean in a number of different ways. The Asian Monsoon System (which is itself influenced by such high-latitude cool episodes) plays an important role, by transferring these in a way which allows them to exert an effective influence on the coupled ocean-atmosphere system.. Thus the close connection of the ENSO development to the annual cycle is principally due to its coupling with the monsoon system.

During recent years, comparatively few papers have been published which focus on possible **extra-tropical** impacts on the tropical climate; these have been mainly concerned with Indian monsoon variability and El Niño/Southern Oscillation events.

Barnett (1985) discusses the cause of an eastward shift of pressure and wind anomalies at sealevel from the equatorial Indian to the

western Pacific ocean to be found in midlatitudes of the Eurasian continent. Krishnamurty et al. (1986) correlated the global pattern of surface pressure with ENSO indices and found comparable results to Barnett (1985). Yasunari (1987) also showed global analyses of bandpass-filtered climatic elements for a relatively short period (1964-81) and stressed the role of midlatitudes of the northern hemisphere. In particular the old idea of the influence of Eurasian snowcover (Blanford, 1884) on the Indian monsoon (and ENSO) could be supported by observations (Hahn and Shukla, 1976; Dickson, 1984 ; Yasunari, 1987) and model calculations (Barnett et al., 1988, 1989). Here an attempt is being made to link those climate anomalies in middle latitudes of the Eurasian continent to external forcing like enhanced stratospheric aerosol or polar stratospheric clouds which reduce the incoming solar radiation in very high latitudes. This provides a test for the hypothesis (Graf, 1985, 1986) that the occurence of ENSO and weak Indian monsoon is triggered by northern hemispheric cooling episodes.

2. Observational Evidence

The course of a Southern Oscillation index (West Pacific rain index following Wright, 1984) is shown in Figure 1, starting in years with temporarily enhanced optical depth in middle latitudes of the Northern Hemisphere (Kondrat'jev, 1985), through the following two years. It is obvious that, independent of the value of the index at the start of the year with enhanced optical depth, the index reaches maximum values (i.e. ENSO-event-values) at the end of year +1 with but two exceptions: 1907 and 1968.

A cross-spectral analysis (Graf, 1985) has shown that, in the spectral band of the Southern Oscillation (3 to 4 years), negative anomalies of the northern hemispheric mean surface air temperature (Jones et al., 1982) precede negative anomalies of the Southern Oscillation by about 12 months.

Since it can not be expected that simply zonal or hemispheric means of air temperature may be used to discover close relationships with the tropical climate variability, correlation patterns for the whole northern hemisphere for near surface temperature and Darwin pressure (serving as Southern Oscillation Index) have been computed. The temperature data were provided by Dr. P. Jones from

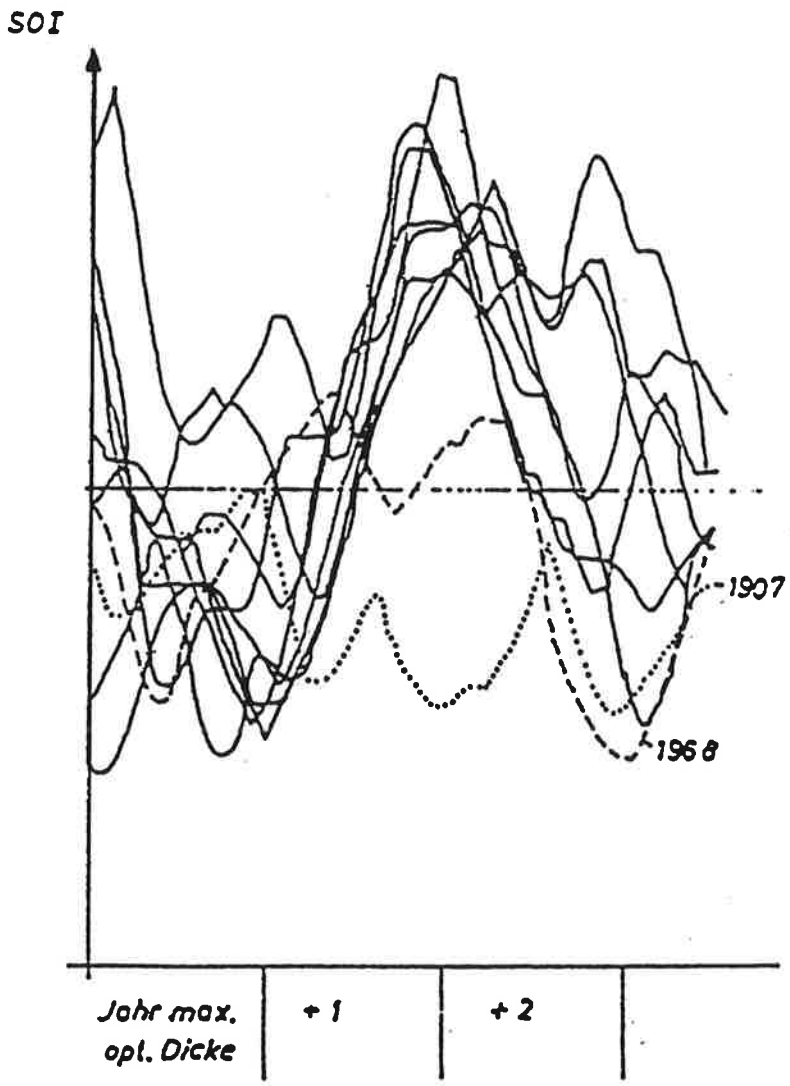

Figure 1: The Southern Oscillation (Rain-Index after Wright, 1984) after relative maxima of optical depth (years 1903, 07, 12, 17, 24, 29, 46, 56 64, 68, 75)

Climate Research Unit at University of East Anglia, Norwich, UK. Darwin pressure data were smoothed by threemonthly running means in order to suppress the strong bi-monthly oscillation in this data set.

Figure 2 shows a sequence of correlation patterns for near surface temperature (see Jones et al. 1989) and Darwin pressure with pressure lagging the temperature by several months. Figure 2a (November temperature , Darwin pressure of February of the over-next year, i.e. 15 months later) shows significant positive correlations between temperature and Darwin pressure over middle and northern Europe as well as over the northern parts of Sibiria. These can be interpreted by intensified zonal circulation due to a cold polar low, which can be found from analyses of the 700 hPa height. An eastward shift of the planetary waves (zonal wave number 2) is also evident (compare Hense, 1986).

Table 1: The occurrence of vorticity and wind anomalies exceeding two local standard deviations (2σ-anomalies) in pre-ENSO winters. Area and element under consideration are indicated in the headlines of the matrices. A cross in the matrix means, that in the given month in the given year a 2σ-anomaly was observed. At the bottom of the matrixes the total number of months with 2σ-anomalies is indicated for pre-ENSO (P), ENSO (E) and remaining years (R) of the period 1956 through 1982.

a) cyclonic 42-72N, 15-85E

month	O	N	D	J	F	M
winter						
1956/7		x				x
1962/3	x	x	x	x	x	x
1964/5	x	x		x	x	
1968/9		x	x	x	x	
1971/2			x	x		x
1975/6		x		x	x	x
1981/2	x	x	x	x	x	x

total: P 29
E 7
R 8

b)anticycl. 42-72N, 175-135W

month	O	N	D	J	F	M
winter						
1956/7	x		x	x		
1962/3	x	x	x	x	x	x
1964/5	x		x		x	x
1968/9				x	x	
1971/2			x		x	
1975/6	x		x			
1981/2				x		

total: P 20
E 11
R 8

c) westerly 42-72N, 45-135E

month	O	N	D	J	F	M
winter						
1956/7			x			
1962/3					x	x
1964/5	x					
1968/9		x		x	x	
1971/2		x	x	x		x
1975/6	x	x	x			
1981/2			x			

total: P 16
E 4
R 5

An analysis of strong anomalies of the relative vorticity and wind components in the middle troposphere (Graf 1989) clearly shows that in pre-ENSO winters cyclonic vorticity anomalies centered over the Ural mountains are preferentially associated with westwind anomalies extending from eastern Europe to central Siberia. Anti-cyclonic vorticity anomalies are also observed in pre-ENSO winters

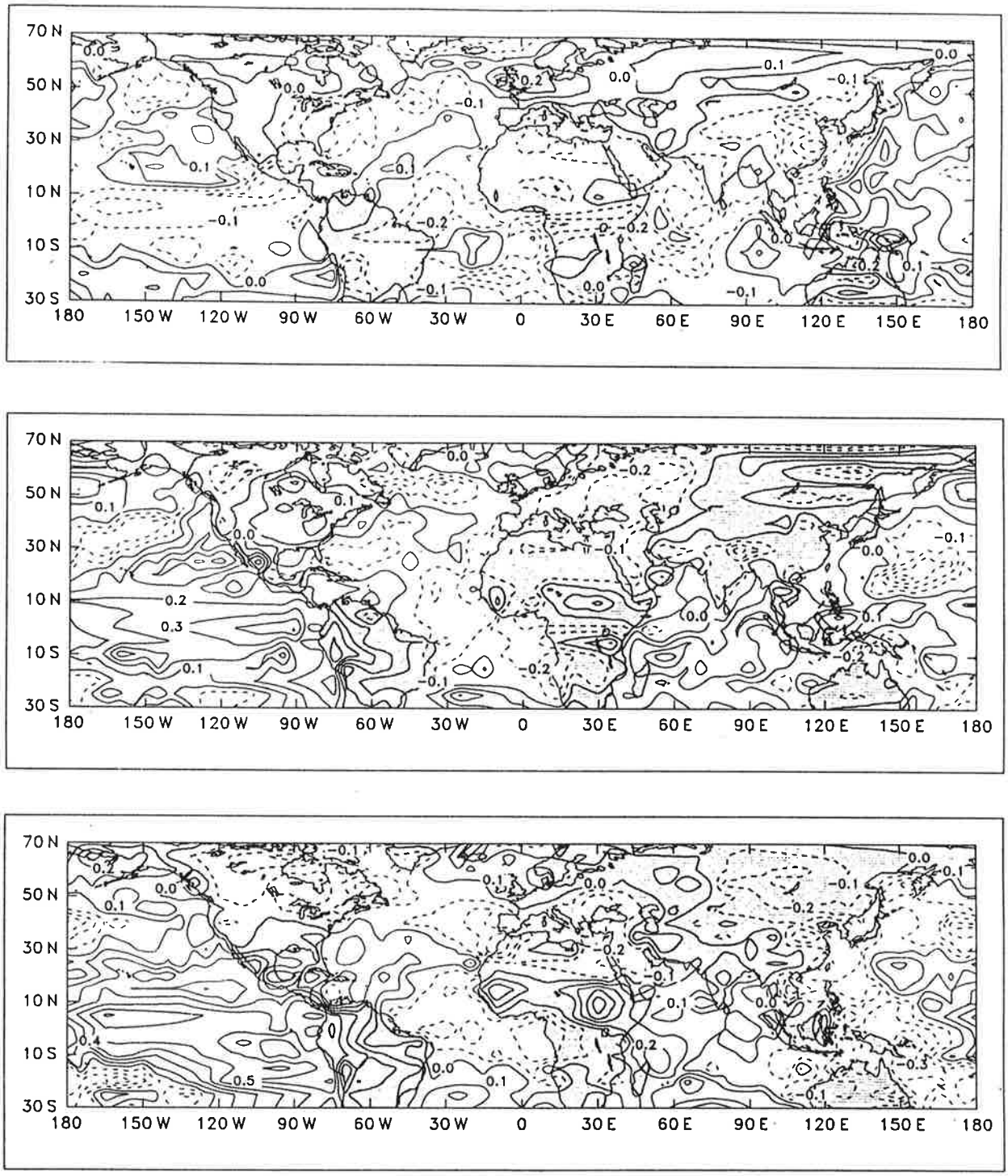

Figure 2: Correlation between near-surface temperature field (1900–1982) and Darwin pressure (three monthly running means), pressure lagging, contour interval 0.1, no zero line, positive (negative) correlation solid (dashed) lines

a) Temperature November, pressure February +2 (central month), lag=15 months

b) Temperature May, pressure February +1, lag=9 months

c) Temperature July, pressure February +1, lag=7 months

in the vicinity of the Aleutean low (Table 1). This result is in good agreement with the findings of Emery and Hamilton (1985) and may contribute to the explanation of the significant negative correlation between temperature and Darwin pressure at the southern East coast of the U.S.A. These cold pre-ENSO winter conditions are due to advection of polar air masses at the western flanc of a North American trough. Similar conditions occur downstream of the Asian high mountains with a cold center over eastern China.

An area of significant positive correlation between air temperature and Darwin pressure is evident over sea between 120^{o}E and 150^{o}E between 10^{o} North and South. This area experiences warming in the phase of building up a water surplus (creation of potential energy) of the ENSO cycle.

It can be expected that with the advection of warm maritime air masses to the eurasian mainland go along enhanced cloudiness and precipitation, which, due to the low temperatue, will build up a deeper than normal snow cover especially at the slopes of the Asian highlands. During the melting period negative temperature anomalies then develop. This is shown in Figure 2b by the negative correlations over eastern Europe that reach from Novaja Semlja via the Ural mountains and the Caspian see to the highlands of Asia. This fits well to the results of Graf (1989) for correlations of 500 hPa heights with Southern Oscillation Index. Figure 3 displays results of a field correlation analysis between the 500 hPa height in April and SOI (surface pressure Tahiti minus Darwin) of the mean of following November through January. Here positive correlations (+) mean a negative height anomaly preceeding negative SOI. Only correlation coefficients above 95% of confidence are indicated by the signs, and for more than 99% of confidence the value of the correlation coefficient is given. The figure shows significant negative pre-ENSO height anomalies over the western part of the Asian Highlands, over the pole (this one is even more pronounced in the 700 hPa level) and in the vicinity of the West Pacific High.

Positive pre-ENSO height anomalies are found over East Asia, indicating strong anticyclonic winter monsoon conditions.

Over North America the correlation coefficients also change their

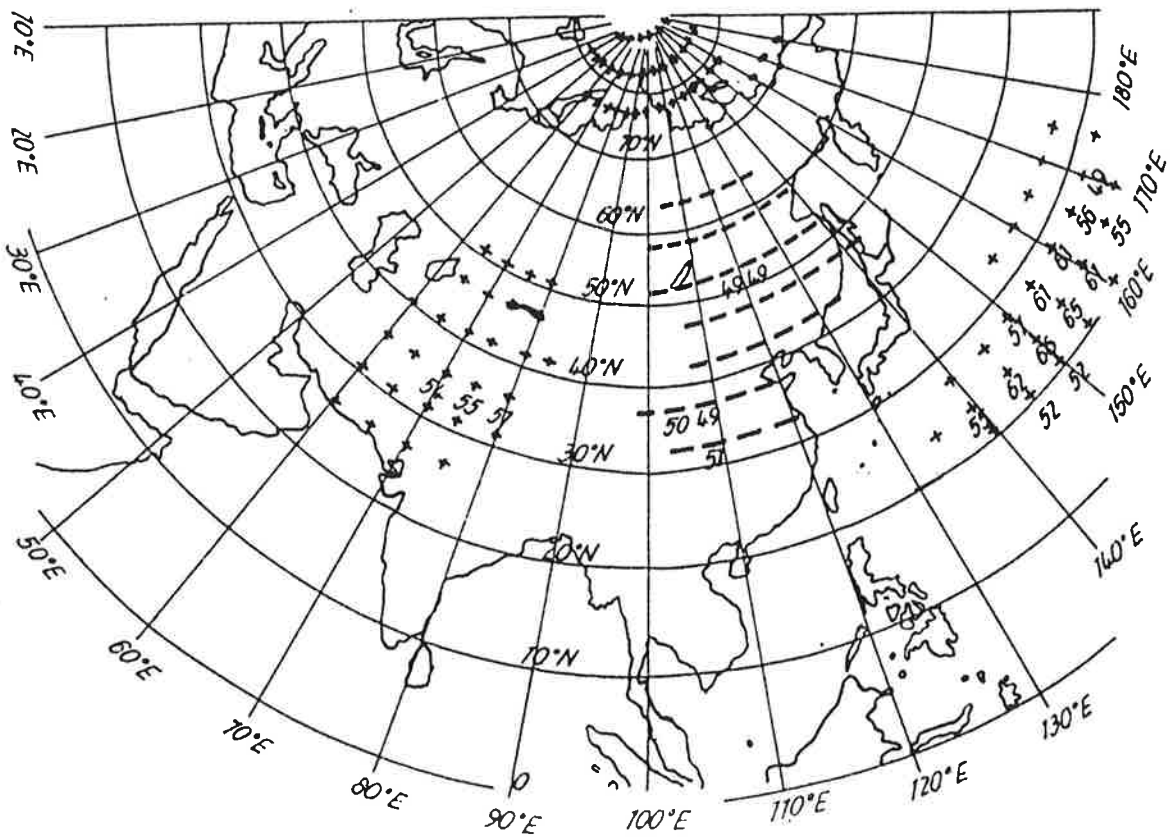

Figure 3: Correlation pattern between the height of the 500 hPa level of April with the mean of the Southern Oscillation Index (Tahiti minus Darwin) for November through January, i.e. SOI lagging 8 months

sign from November to May. While there were cold conditions at the east coast in fall, now, in late spring, warm temperatures occur in ENSO year "0". One reason for this swich in sign may be less than normal snow in the pre-ENSO winter east of the Rocky Mountains (see e.g. Yasunari, 1987) due to the dryness of the arctic air that was advected in winter.

In the El Niño region of eastern equatorial Pacific positive significant correlations develop which are a first signal for warming up of this area in spring of the ENSO year.

Figure 2 c represents the correlation pattern of July temperatures versus the Darwin pressure of February. Outstandingly high positive correlation coefficients of up to 0.6 develop over the El Niño area indicating the further development of warming of the eastern tropical Pacific ocean.

The positive correlations between temperature and Darwin pressure in the Indian monsoon region and over equatorial North Africa mirrors the close connection between Southern Oscillation and monsoon. The higher temperatures in ENSO year 0 are due to less precipitation and cloudiness. Low temperatures appeare in summer of the ENSO year "0" over the western equatorial Pacific. This significant anomaly is produced by enhanced rainfall and cloudiness and represents the "counter monsoon trough" that was discussed by Graf (1987).

The low temperatures in mid-latitudes of Asia are consistent with the "prolonged winter monsoon conditions" which have been discussed in terms of field correlations between SOI and geopotential heights in Graf (1989). They describe the cold air reservoir that feeds the cold air outbreakes with northerly wind anomalies over the tropical West Pacific.

Graf (1986, 1987a) has presented some evidence for the frequent coincidence of volcanic eruptions (especially in high northern latitudes) with subsequent ENSO episodes. One of the generally accepted climatic effects of stratospheric aerosol injection is the reduction of the global (direct plus diffusive) radiation in high

latitudes by an order of 5% at El Chichon type eruptions (e.g. Kondrat'jev (1985), McCracken and Luther (1984), Mass and Portman (1987)). This radiation deficit is argued to be *one* possible external forcing factor for the above-mentioned climatic anomalies associated with ENSO events. To test this hypothesis, the effect of high-latitude radiational forcing was examined in a GCM experiment.

3. The Model

The atmospheric General Circulation Model used for the experiment described is the T21 low resolution spectral forecast model of the European Centre for Medium Range Weather Forecasts (ECMWF). Its performance in describing the observed climate has been shown in previous Reports (Fischer, 1987; Fischer, 1989; von Storch, 1988).
For a brief description see also Barnett et al. (1989).The actual version used here is "Cycle 28". This is similar to the "Cycle 24" version (see Dümenil and Schlese,1987b) with one important difference relating to the albedo of the snow cover. In the versions prior to Cycle 28 the albedo of snow-covered land was always 60%, while in Cycle 28 thawing snow cover now has an albedo of 40%.. This change made the model's climate warmer and thus brought it closer to the observed climate.
The main differences of Cycle 28 relative to "Cycle 17" (Dümenil and Schlese, 1987a) are the introduction of the Kuo scheme (which describes multiple layer clouds without an ice phase, and in which the cloud base is calculated from surface conditions), a shallow convection scheme (which allows vertical transports in convectively unstable layers), a fast exponential sum-fitting technique for the longwave part of the radiation scheme, and a new cloud cover prediction scheme (low, medium and high clouds are functions of relative humidity, convective activity, inversion strength and vertical velocity).

4. The Experiment

The model experiment is an attempt to simulate a strong eruption of an explosive volcano in high latitudes of the Northern Hemisphere (e.g. in Kamchatka, the Aleutian Islands, the northern Rocky

Mountains or Iceland) in Spring. Several months after the eruption the sulphuric aerosol will be fully developed and persist at high latitudes. This will cause a reduction of the global radiation in latitudes north of the volcano. Given the physical scheme of the T21 GCM, the only simple way to simulate such a perturbation is to reduce the incoming solar shortwave radiation at the top of the atmosphere. Thus the following reductions were introduced as the radiational forcing (Table 2).

Table 2: Reduction (%) of the incoming shortwave solar radiation at the top of the atmosphere for the experiment VOLEX '88

Lat.°	<52.61	52.61	58.14	63.68	69.21	74.74	80.27	85.76
Reduction	0	2	4	6	8	10	10	10

All other parameters of the model remained unchanged. SST was climatologically prescribed. The control experiment consists of a 5 year run with the full annual insolation cycle but no daily cycle. The radiation anomaly was switched on at year 3 of the control run in June and was held constant for 14 months, i.e. through August of the following (+1) year. There have been run three experiments each of 14 months duration, with independent initial conditions, and a fourth experiment in which the radiation anomaly was switched off in February of year +1. The results of the model experiment will be shown mainly as means of the three independent model runs, mostly normalized by the local standard deviation of the model climate. All anomalies were observed in all individual runs. The effect of switching off the radiation anomaly in February +1 will be discussed in the appendix.

5. Results

The response of the T21-Atmosphere to the radiation anomaly is presented in standardized terms, i.e. relative to the local variability of the control run climate (Lautenschlager, 1988). This provides a simple means of estimating the significance of the anomalies. Since the experiment was mainly directed towards testing

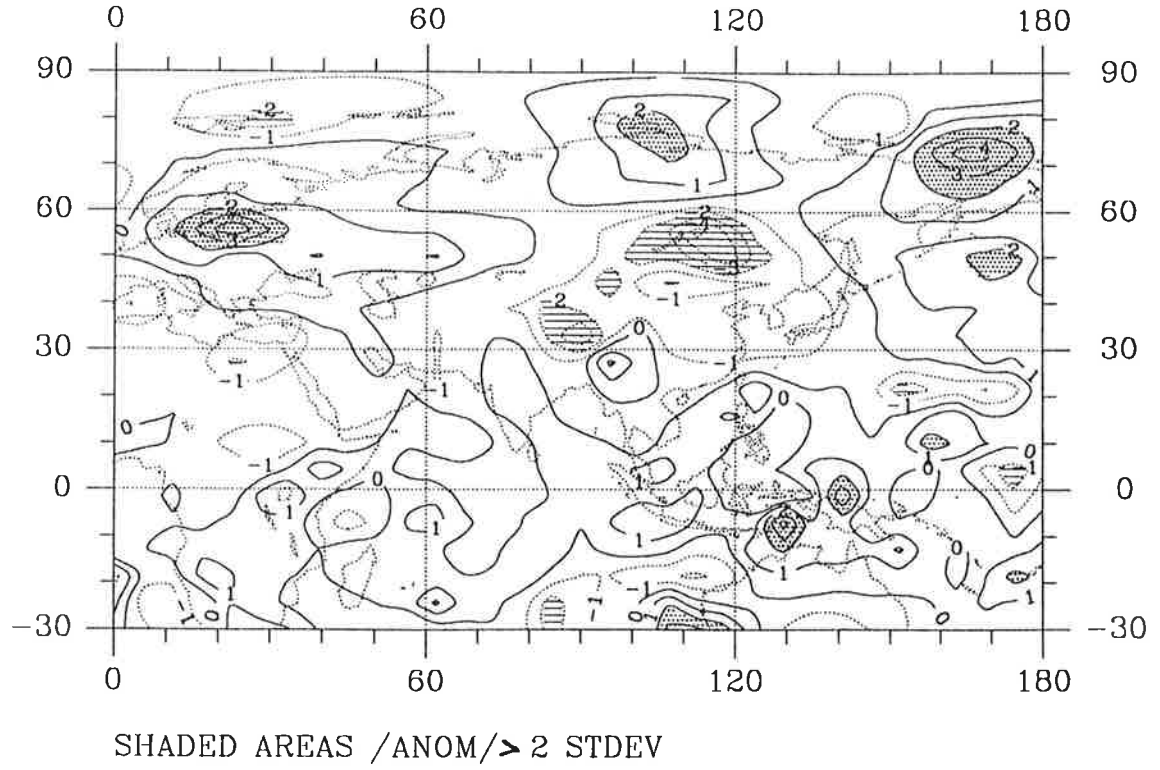

Figure 4: Mean anomaly of the 2m-temperature from three independent AGCM experiments with reduced insolation over the northern polar cap. Anomalies normalized to local standard deviations, November of year 0.

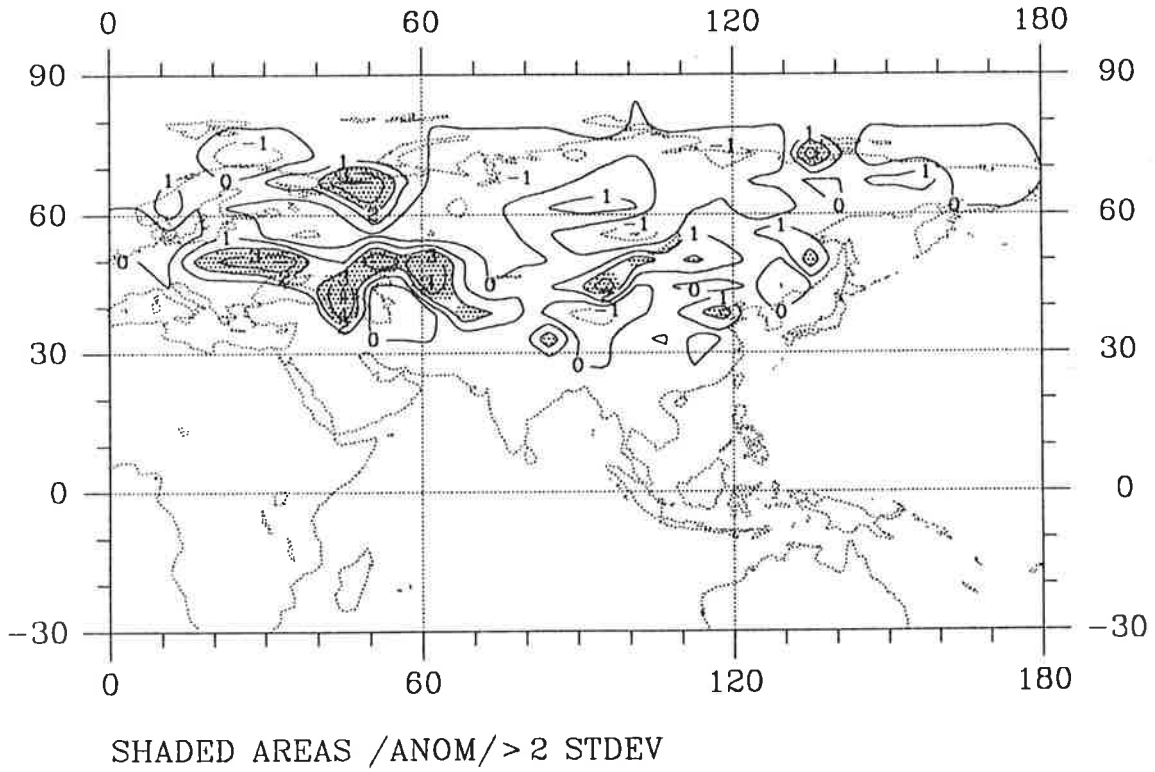

Figure 5: As Figure 4, but snow depth in March+1.

the hypothesis that cooling the northern high latitudes may lead to weak Indian monsoon and ENSO, the presentation of the results is restricted to the eurasian co n tinent and , for the lower tropospheric wind, to the tropical Pacific ocean.

In general, anomalies of the free atmosphere in fall and winter are not very continuous either temporally or spatially. Much more continuous anomalies in these seasons are connected with the soil temperature, and hence the energy balance of the earth's surface. In Figure 4 for November of year 0 (i.e. 5 months after the introduction of the radiation anomaly) positive temperature anomalies evolve over central Europe, extending to Kazakhstan. This pattern holds for the whole of fall and winter. The positive temperature anomaly extends to northern Siberia and may be interpreted as the result of the advection of moist air from the Atlantic region. The same holds for the positive temperature anomaly along the northern Pacific coast of Asia. Here the source of moist air comes from the Pacific ocean and the flow is due to anticyclonal circulation anomalies in this area.

Extended negative temperature anomalies develop right over Tibet and over Mongolia and the Baikal region. Thus, over the Eurasian con tinent the temperature anomaly pattern for fall is very similar to the temperature pattern that can be developed for fall of year -1 in the ENSO cycle from Figure 2a. Of greatest importance for the further development of the climatic anomalies are the snowfall and snowcover anomalies, which are very robust and lead to an increased persistence of the initial disturbance. The snowfall is enhanced from November through the spring of the next year, mainly in the area south of the radiation anomaly over Asia. In North America there is a tendency towards a reduction in snowfall, especially north of the polar circle. The same is true for the West Siberian Lowlands in the lee of the Ural Mountains.

The snowfall and snowcover patterns (e.g. March, Figure 4) are closely linked to the orography, with positive anomalies at the western flanks of orographic barriers, e.g. Scandinavia, the Alps and the Asian mountains (e.g., Caucasus, highlands of Iran, Tien Shan, etc.). The amount of additional snow is in the range of 10 to 15 cm water equivalent, which corresponds to 40 to 60 centimeters of aged snow, an amount which is approximately 50 percent of the climatological snowcover in the most sensitive areas. The snow

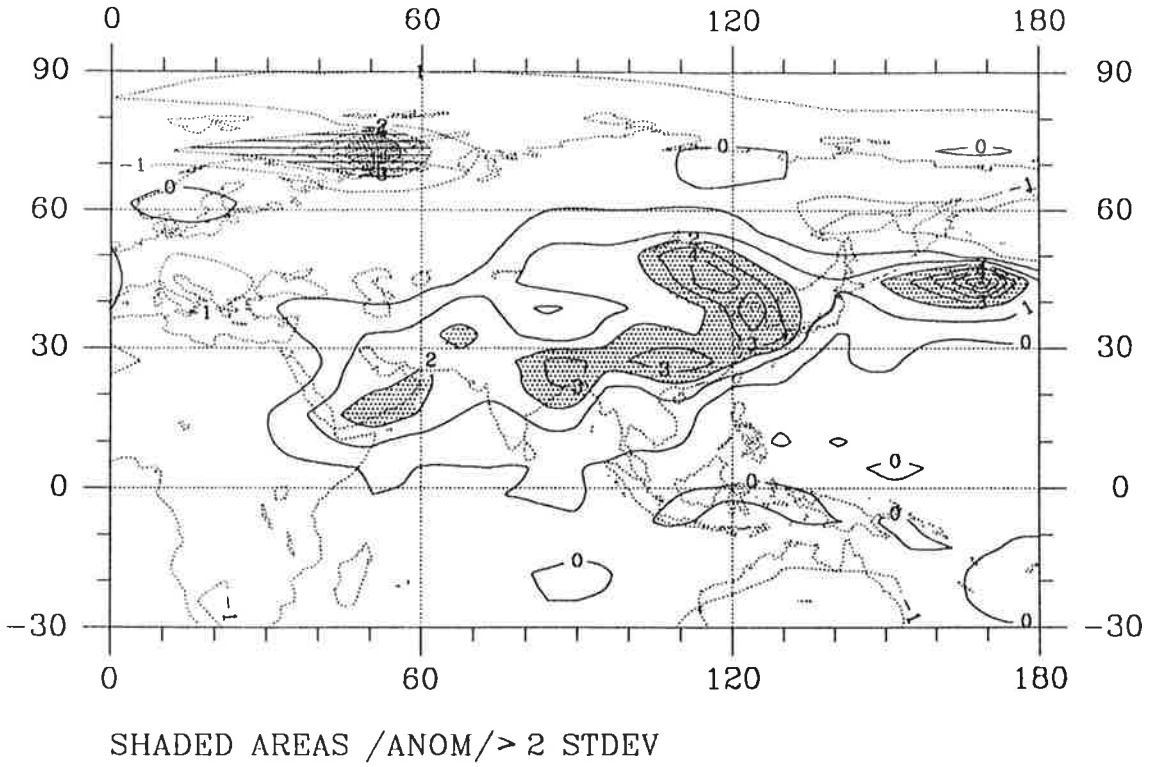

Figure 6: As Figure 4, but surface pressure in May+1.

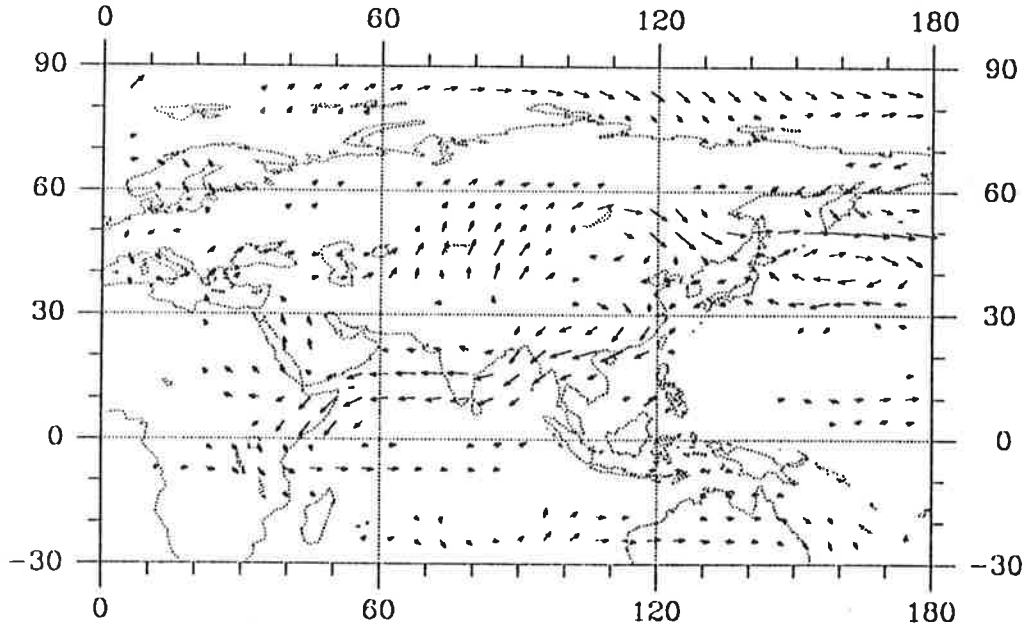

Figure 7: As Figure 4, but wind vector 850 hPa in May+1, unnormalized, for Eurasia.

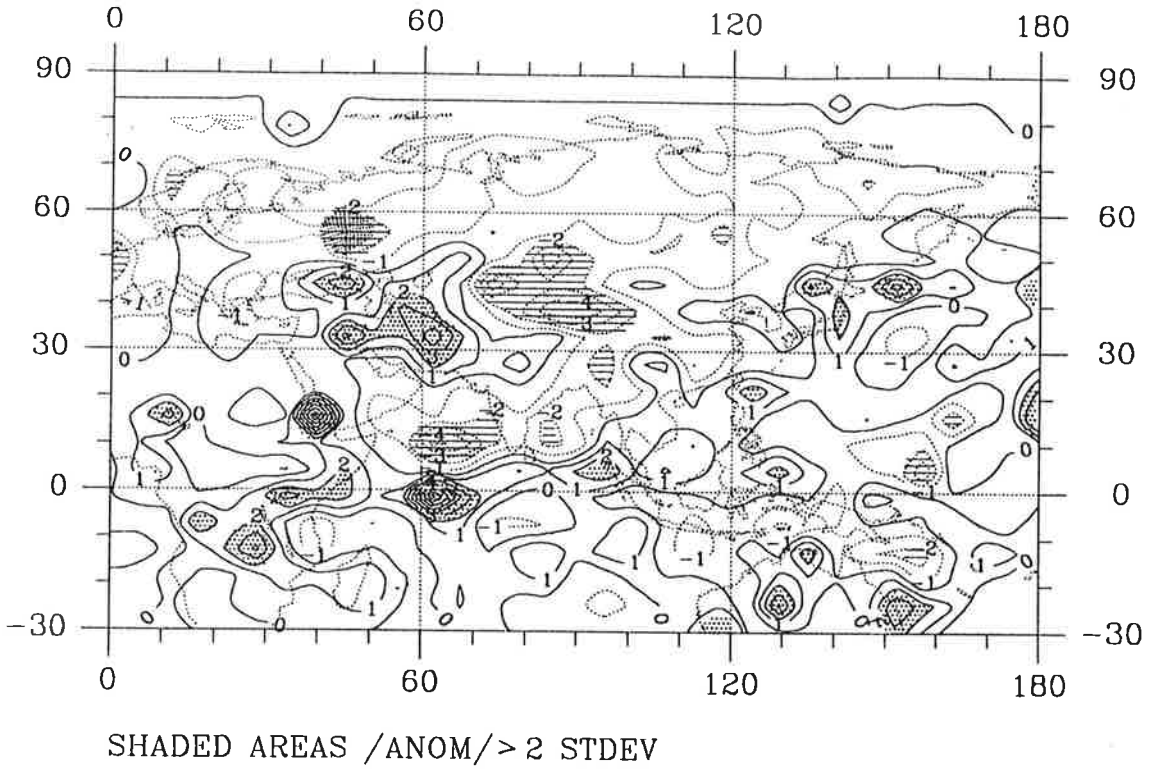

Figure 8: As Figure 4, but convective rainfall in May+1.

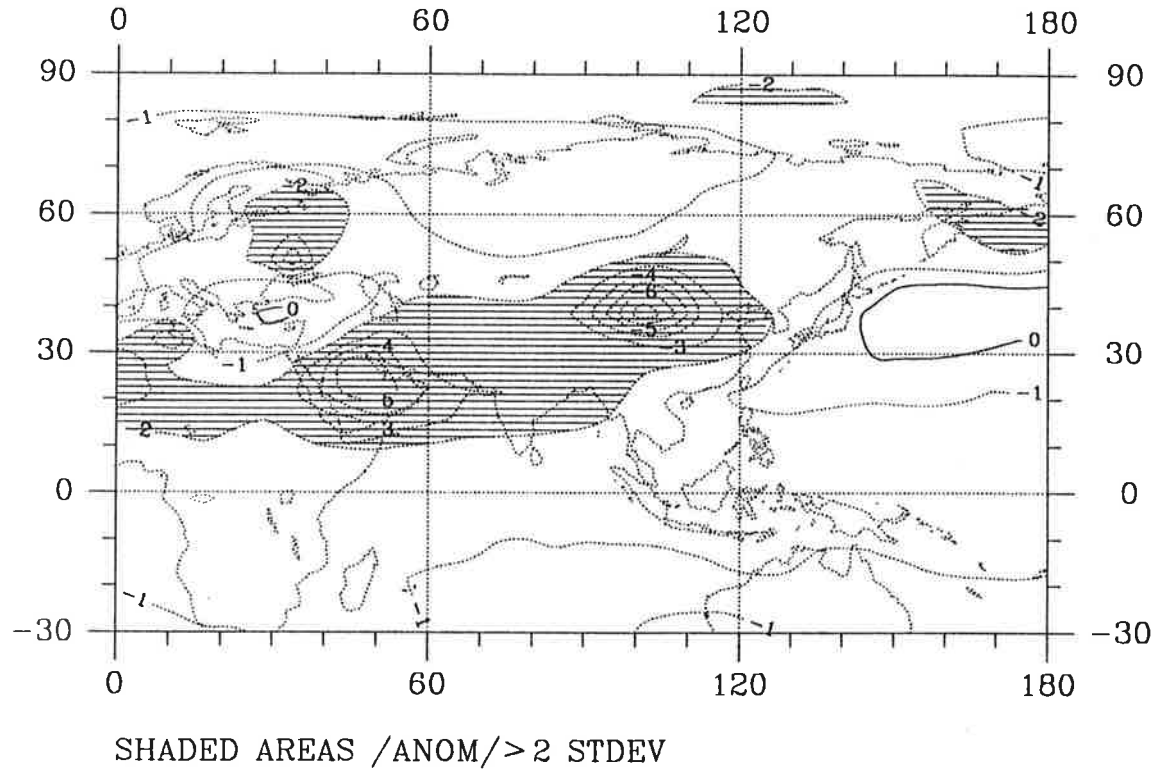

Figure 9: As Figure 4, but geopotential of 200 hPa level in May+1.

anomaly patterns, especially west of 60°E are very similar to those obtained by Yasunari (1987b) for the transitional phase from anti-ENSO to ENSO.

The model response to the initial radiation anomaly in May is dominated by a strong high pressure anomaly (Figure 6) over East Asia and in the Indian monsoon region. This anomaly represents a prolonged winter monsoon anomaly, as can easily be seen from the mean wind vector anomaly in the 850 hPa level (Figure 7). This result also corresponds with earlier suggestions (Graf, 1986, 1987 a,b) and correlation analyses between the 500 hPa level and the Southern Oscillation Index by Graf (1989). The northeasterly wind anomalies at the Horn of Africa (implying a weakened Somali-jet) are characteristic of a year of weak Indian monsoon (Findlater,1971) as are the westwind anomalies at the equatorial Indian ocean (Gutzler and Harrison, 1987). Figure 8 shows extended negative precipitation anomalies in the region where the NE monsoon anomaly occurs, as well as over Tibet. The missing convective rain in higher latitudes is evidently due to the radiation anomaly. Some enhanced precipitation is seen in the equatorial area, pointing to a southward shift of the Intertropical Convergence Zone. This is to be expected with increased hemispheric meridional temperature gradient (e.g. Korff and Flohn, 1969, Graf, 1986). The reduced heating of the troposphere, due to decreased rainfall, results in negative anomalies of the height of the 200 hPa level over much of subtropical Asia (Figure 9).

Contemporarily with the NE monsoon anomaly over the tropical Pacific ocean, a weakened Walker circulation is evident (Figure 10). The strongest west wind anomalies appear at the position of the North Equatorial Countercurrent (between 3 and 8°N) in the western Pacific and right over the equator in the eastern part of the ocean. The magnitude of these westwind anomalies is of the order of 1.5 to 2 m/s. The southeast trades in the eastern part of the Pacific are greatly weakened with maximum reduction of 4 to 5 m/s at 20°S. These circulation anomalies may well be able to trigger El Niño events, provided potential anomaly is created in the western equatorial Pacific (warm water surplus, positive sea level anomaly). The possibility that El Niño might be triggered by westwind anomalies of such a magnitude has been shown with a coupled model of tropical Ocean and Atmosphere by Latif et al. (1988) and Barnett et al. (1989).

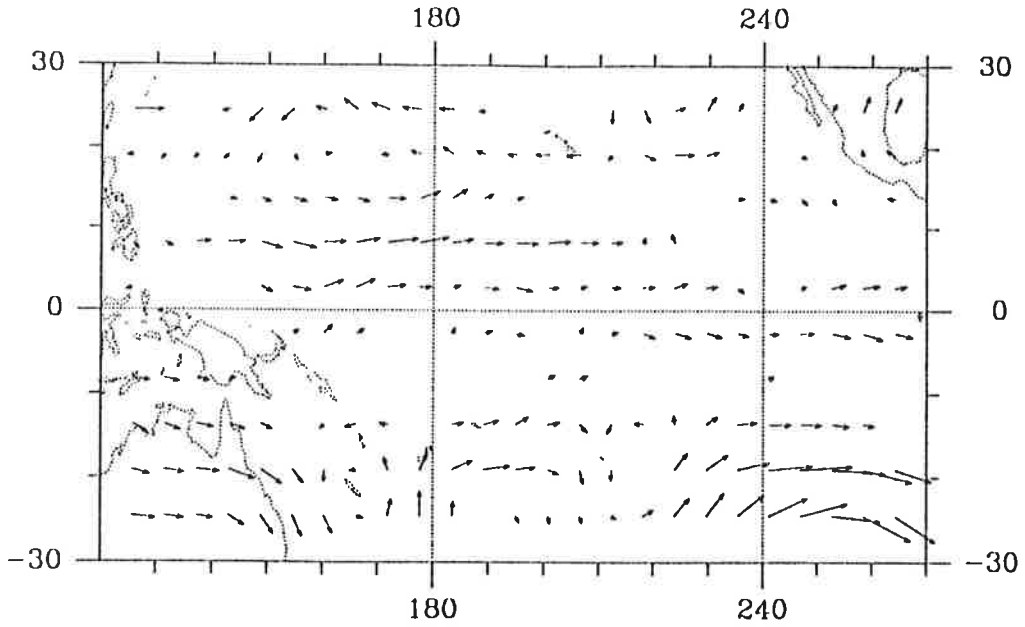

Figure 10: As Figure 4, but wind vector 850 hPa in May+1, unnormalized, for tropical Pacific.

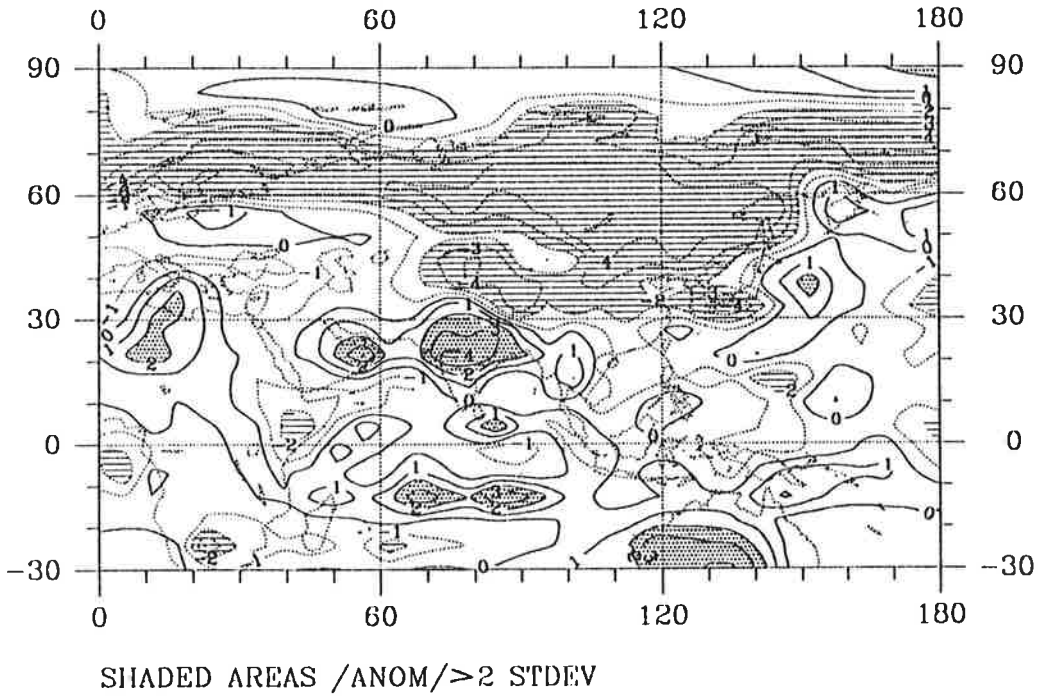

Figure 11: As Figure 4, but 2m-Temperature for June+1.

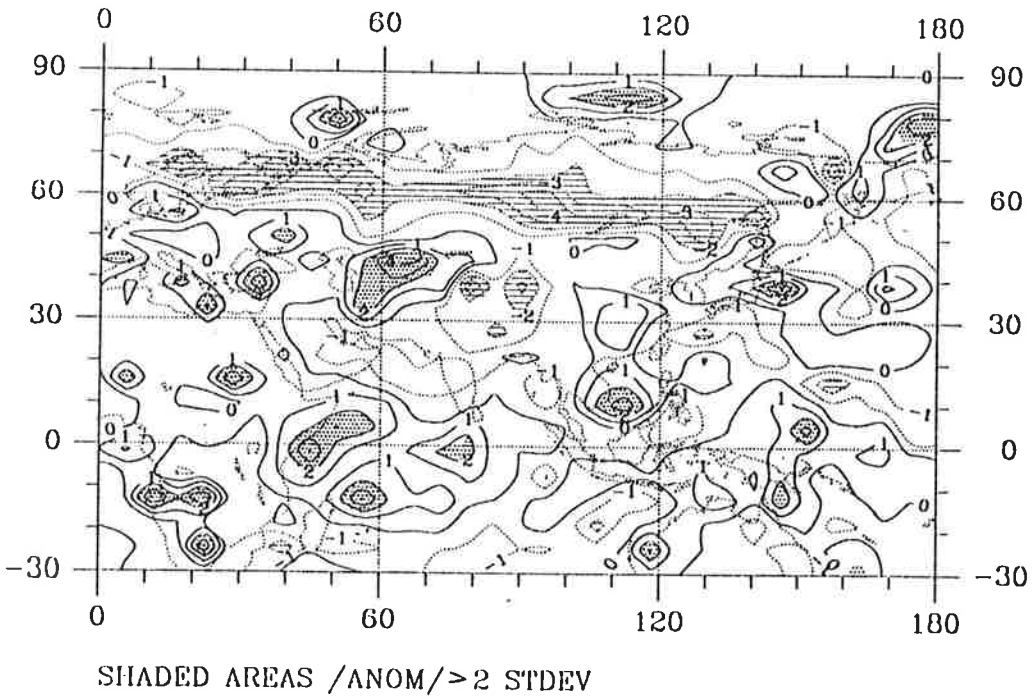

Figure 12: As Figure 4, but convective rainfall in June+1.

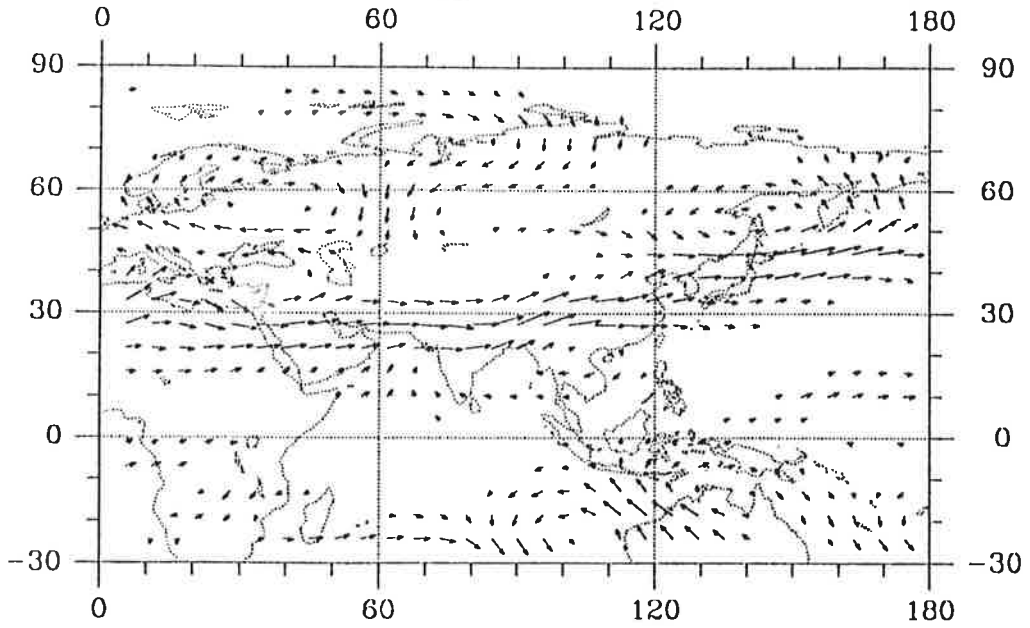

Figure 13: As Figure 4, but wind vector 200 hPa in June+1, unnormalized

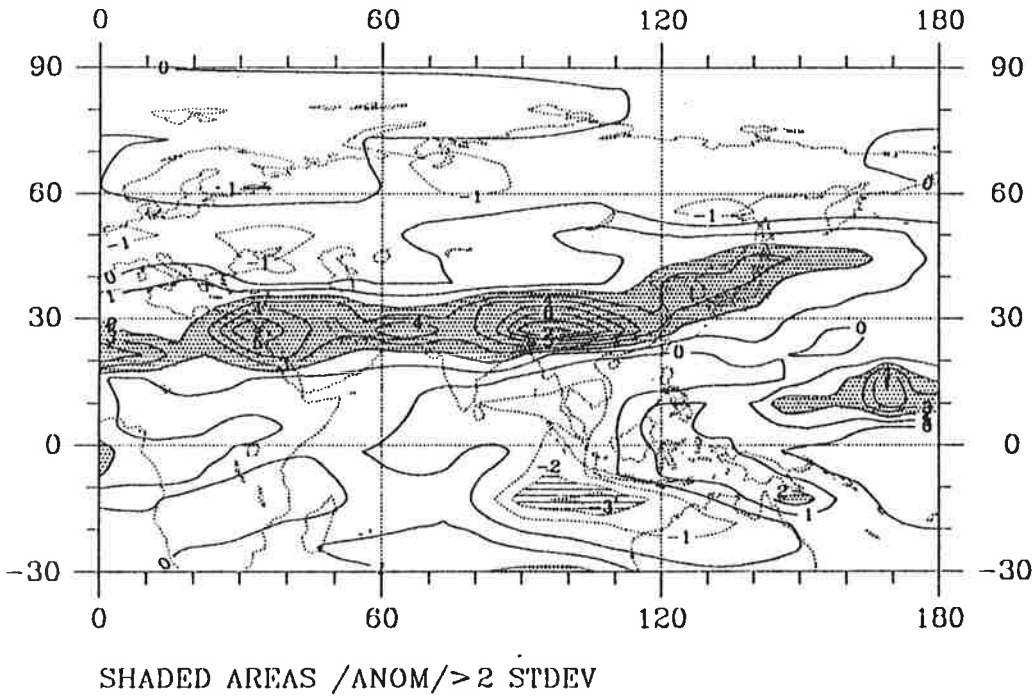

Figure 14: As Figure 4, but for zonal wind component 200 hPa Jun+1

In June (besides the negative temperature anomalies north of 50°N, which are due to the still existent insulation deficit) cold temperatures occur over East and Southeast Asia (Figure 11). This pattern fits extraordinarily well with ENSO summer (year 0) temperatures that can be constructed from Figure 2c. The positive temperature anomaly over India at the surface is obviously due to less cloudiness and less soil moisture resulting from weak monsoon rains (Figure 12). The reduced latent heating of the troposphere finally leads to a strongly reduced (in the order of 10 m/s) easterly jet in the upper troposphere south of the Himalayas (Figures 13 and 14). This reduction of the "monsoon-jet" is a highly conclusive result and makes the reduction of large scale Indian monsoon evident.

6. Conclusion

The model experiment was conceived in order to test the hypothesis that a radiation deficit in higher northern latitudes, reflecting the effects of volcanic eruptions (or polar stratospheric clouds!) may generate conditions which are favourable for a weak Asian summer monsoon and for triggering El Niño events. The experiment was run with a rather simple and strong perturbation - the persistent reduction of incoming radiation at the top of the model atmosphere, up to 10% in high northern latitudes. The results provide physically-consistent evidence in support of this basic hypothesis. The main supporting factor is the creation of enhanced snow cover in regions of Asia which are removed from the latitudinal belt of the introduced radiation anomaly. As expected, it is mainly the mountainous regions which receive more snow than normal.The additional snow amount is of the order of 10 to 15 cm water equivalent, which is similar to the "a priori" snow anomaly introduced in the recent experiment by Barnett et al. (1987, 1989). The difference relative to the present experiment is that Barnett et al. multiplied (or halved) the falling snow by a factor of two, while our approach allowed snow to respond directly to the radiative forcing in a physically realistic way. Some of the simulated features are in better accord with observational evidence than in the Barnett et al. experiment (e.g., the warm near surface anomalies for June after a winter with "much snow" , cf. Fig. 11,

over India and Europe, which did not appear in their experiment).
The model results show certain features, which are well known from observations in weak monsoon years, i.e. the weakened easterly jet in the upper troposphere over northern India, prolonged winter monsoon conditions and prevailing anticyclonal vorticity anomalies over the entire Indian summer monsoon region. Over the western Pacific at the end of boreal winter (May), increased convective activity leads to a negative Walker Circulation anomaly, with westerly wind anomalies near the surface and easterly anomalies in the upper troposphere. Together with the cyclonic vorticity anomaly, this might be interpreted as the "counter monsoon trough" (Graf, 1986,1987 a,b), which takes over the role of the Indian summer monsoon trough. The westerly wind anomalies near the surface may then act as supportive triggers for El Niño.
The results for the Asian Monsoon region are in good agreement with the basic hypothesis. It should be stressed, however, that keeping the ocean temperature at a "climatic" level and also prescribing the sea-ice extent in polar latitudes will, after a few months, lead to a highly imbalanced system especially in high latitudes. Thus, additional experiments with coupled models (at least using a simple energy balance/mixing layer ocean) should be run to overcome these shortcomings.

Acknowledgements

The author appreciates the assistance of D. Schriever and the staff of the Max-Planck-Institut for Meteorology. Their patient support of this work, including discussions with H. von Storch, is greatly acknowledged. Figure 2 was kindly produced by B. Santer. The work was financially supported by the Deutscher Akademischer Austauschdienst and by the Max-Planck-Gesellschaft.

Literature

Blanford,H.F., 1884: On the connexion of Himalayan snowfall and seasons of drought in India. Proc. Roy.Soc. of London 37, 3-22

Barnett,T.P., 1985: Variations in near-global sea level pressure. J.Atmos.Sci.42, 478-501

Barnett,T.P.; Dümenil,L.; Schlese,U.; Roeckner,E., 1987: The effect of eurasian snow cover on global climate. Science, 239, 29 Jan, 504-507

Barnett,T.P.; Dümenil,L.; Schlese,U.; Roeckner,E., Latif,M. 1989: The effect of eurasian snow cover on regional and global climate. Journ.Atmosph.Sci.,46, 661-685

Blanford,H.F., 1884: On the connexion of Himalayan snowfall and seasons of drought in India. Proc. Roy.Soc. of London 37, 3-22

Dickson,R.R., 1984: Eurasian snow cover versus Indian summer monsoon raifall - An extension of the Hahn-Shukla results. J.Appl.Met.23, 171-173

Dümenil,L.; Schlese,U., 1987a: Description of the General Circulation Model. In: Fischer (ed.), Climatic Simulations with the ECMWF T21 model in Hamburg. Large Scale Atmospheric Modeling, Rpt. No.1, 3-10

Dümenil,L.;Schlese,U., 1987b: Changes to the Parameterisation package and their impact on perpetual January Simulations. In: G.Fischer (ed.) Climatic Simulations with the ECMWF T21 model in Hamburg. Large Scale Atmospheric Modeling, Rpt. No.1, 3-10

Emery,W.J.; Hamilton,K., 1986: Atmospheric forcing of interannual variability in the northeast Pacific ocean: Connections with El Niño. Journ.Geophys.Res. 90, 857-868

Findlater, J., 1971: Mean monthly air flow at low levels over the Western Indian Ocean. Geophysical Memoirs, 115, H.M.S.O., London, 53 pp

Fischer,G. (ed.), 1987: Climate simulations with the ECMWF T21-model in Hamburg. Meteorolog.Inst.Univ. Hamburg, Large scale atmospheric modeling, Rept.No.1

Graf,H.F., 1985a: Eine globale Eigenschwingung des Systems Ozean-Atmosphäre. Z.Meteorol. 35, 223-226

Graf,H.F., 1986a: On El Niño/Southern Oscillation and northern hemispheric temperature. Gerlands Beitr.Geophys. 95, 63-75

Graf,H.F., 1986b: On the coincidence of explosive volcanic eruptions with El Niño/Southern Oscillation events. Proc. 1st WMO-Conference on Long-Range Forecasting, Sofia, Sept.29 - Oct.3, 1986 (WMO, Geneva).

Graf,H.F. 1987: Some evidence for a northern hemispheric extra-tropic trigger mechanism of ENSO events. In Proc. 12th Annual

Climate Diagnostics Workshop, Oct.1987, Salt Lake City, UT, 200-209

Graf,H.F., 1989: Associations of relative vorticity and wind anomalies over the northern hemisphere with the ENSO-cycle. subm. to Contr.Phys.Atm., Jun.1989

Graf,H.F., 1989: The middle troposphere over Asia prior and during El Niño/Southern Oscillation events. Z.Meteorol., 39,

Gutzler,D.S.; Harrison,D.E., 1987: The structure and evolution of seasonal wind anomalies over the near equatorial eastern Indian and western Pacific oceans. Mon.Wea.Rev.115, 169-192

Hahn,D.G.; Shukla,J., 1976: An apparent relationship between Eurasian snow cover and Indian summer monsoon rainfall. Journ.Atmos.Sci. 33, 2461-2462

Hense, A., 1986: Multivariate statistical investigations of the northern hemisphere circulation durinng the El Niño event 1982/83. Tellus 38A, 189-204

Jones,P.D. et al., 1982: Variations in surface air-temperature, Part 1: Northern hemisphere 1880-1980. Mon.Wea.Rev. 110, 59-70

Jones, P.D.; Wigley, T.M.L.; Farmer, G., 1989: Marine and land temperature data sets: A comparisonn and a look at recent trends. In: *Proceedings of DOE Workshop on Greenhouse-Gas-Induced Climatic Change* (Ed. M.E. Schlesinger). In press.

Kondrat'jev, K.Ja., 1985: Vulkany i klimat. Itogi nauki i techniki. Meteorol. i klimatol.. t.14. Moskva, VINITI, 204 S.

Korff,A.C.; Flohn.H., 1969: Zusammenhang zwischen dem Temperatur gefälle Aequator - Pol und den planetaren Luftdruckgürteln. Ann.et.N.F.4, 163-164

Krishnamurty,T.N.; Chu,S.H., 1986: On the sea level pressure of the Southern oscillation. Arch.Met.Geoph.Biocl., A34, 385-425

Latif, M.; Bierkamp, J; von Storch, H., 1988: The response of a coupled ocean-atmosphere general circulation model to wind bursts. J. Atmos. Sci. 45, 964-979

Loon,H.,van, 1984: The Southern Oscillation: Prelude on the Southern and finale on the Northern Hemisphere. Studies in Climate, v.Loon (ed.), NCAQR/TN-227+STR, Boulder CO,306-335

Loon,H.,van; Shea,D.J., 1985: The Southern Oscillation. Pt.IV: The precoursors south of 15S to the extremes of the oscillation. Mon.Wea.Rev. 113,2063-2074

Loon,H.,van; Shea,D.J., 1987: The Southern Oscillation.Pt.VI: Anomalies of sea level pressure on the Southern Hemisphere and of Pacific sea surface temperature during the development of a warm event. Mon.Wea.Rev. 115,370-381

Mass,C.F.; Portman,D.A., 1989: Major volcanic eruptions and climate: A critical evaluation. J. Climate, 2, 566-593

McCracken,M.C.; Luther,F.M., 1984: Preliminary estimate of the radiative and climatic effects of the El Chichon eruption. Geofiz.Intern. 23, 385-401

Storch,H.,von; van Loon,H.; Kiladis,G.N., 1987: The Southern Oscillation. Pt.VIII: Model sensitivity to SST anomalies in the tropical and subtropical regions of the South Pacific Convergence Zone. Mon.Wea.Rev. 115, in press

Storch,H.,von (ed.), 1988: Climate simulations with the ECMWF T21-model in Hamburg. Part II: Climatology and sensitivity experiments. Meteorolog.Inst.Univ.Hamburg. Large Scale Atmospheric Modelling Report No.4

Wright,P.B., 1984: Relationships between Indices of the Southern Oscillation. Mon. Wea. Rev. 112, 1913-1919

Yasunari,T., 1987: Global structure of the El Niño/Southern Oscillation.Part II:Time evolution. J.Meteorol.Soc.Japan 65,81- 102